Static and Fatigue Behaviour of Impact Damaged Thick-Walled Composites

Customer

NL Agency

NLR-TP-2013-511 - April 2014

NLR – Dedicated to innovation in aerospace

National Aerospace Laboratory NLR
Anthony Fokkerweg 2
1059 CM Amsterdam
The Netherlands
Tel +31 (0)88 511 3113
www.nlr.nl

EXECUTIVE SUMMARY

Static and Fatigue Behaviour of Impact Damaged Thick-Walled Composites

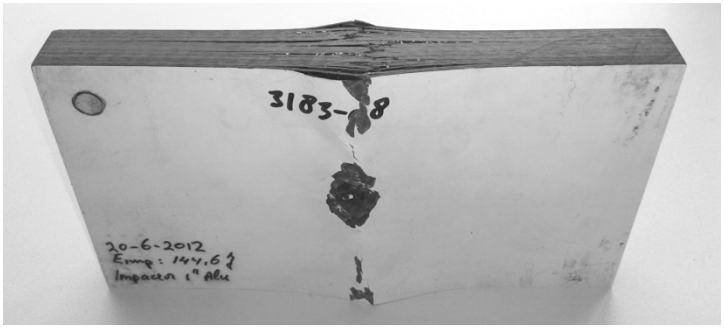

Problem area

One of the critical threats to composite aircraft structures is impact by foreign bodies. A variety of impact threats can be characterised, e.g. tool drop, collision with ground vehicles, hail, runway debris sucked up by engines or thrown up by the tyres. Thick composites, such as applied in highly loaded landing gear components, respond differently to an impact event than thin composites.

Test data from literature and past test results seemed to indicate that aircraft structures made of thick composites material are less vulnerable to impact damage than thin composites. This would allow for the application of higher design strains in thick composite structures. In order to meet the objective of increased design strains for thick composites, it must be shown that the Compression Strength After Impact (CSAI) is higher and that (at the same time) damage growth under fatigue loading does not become critical. Therefore, both the static failure behaviour and the damage growth behaviour under fatigue have been investigated.

Report no.
NLR-TP-2013-511

Author(s)
R.J.C. Creemers
M.J. Smeets

Report classification
UNCLASSIFIED

Date
April 2014

Knowledge area(s)
Aerospace Structures &
Manufacturing Technology

Descriptor(s)
Impact damage
Thick composite
fatigue
landing gear
CAI

This report is based on a presentation held at the RTO Workshop, Riga, Latvia, October 2013

Description of work

Thick structural elements have been impacted using four different impactor shapes. Both high velocity impacts using a gas cannon and low velocity impacts using a guided drop weight tower were performed. After impact application the three most critical configurations were tested statically or in fatigue. Ultrasonic C-scans are used to characterise the initial damage and to detect any damage growth during the fatigue tests. After the fatigue tests slices have been cut from some specimens in order to inspect them with a microscope.

Results and conclusions

The creation of damage due to an impact event is different for thick composites compared to thin composites. The large bending stiffness prevents fibre break-out at the back surface and therefore also the creation of a significant dent at the front surface. Instead, a pit/hole is created right at the impact location where the impactor penetrates the top surface, or alternatively only a very shallow dent occurs in combination with a large amount of internal damage.

Depending on the type of impact, the static strength can be quite low and the objective of increased design strains for thick composites can clearly not be met when using only an external damage visibility criteria. The large amount of internal delamination damage leads to local sub-laminate buckling prior to failure.This results in locally very high (bending) strains in the post-buckled sub-laminates. The high compressive strains in the load-carrying 0° plies are the most likely cause for final failure through fibre kinking/crippling.

Under fatigue loading damage growth initiates in the same mode as final failure in the static test specimens. Again, damage growth starts by fibre kinking of the load-carrying 0° plies within a (post-buckled) sub-laminate. Buckling increases the strains in such a sub-laminate and promotes the initiation of a crack under fatigue loading. Next, this crack grows across the width of the sub-laminate until it reaches the edge of the delaminated area. And finally, the crack and delamination grow together towards the free edge of the specimen.

So, both static and fatigue failure are governed by a fibre-dominated failure mode, and the fatigue strength can be directly related to the static strength with the fatigue limit at a fixed ratio of 60% of the static strength.

Applicability

The results of the research programme can be used for the design and analysis of any thick component to which damage tolerance requirements apply, for instance thick wing skin laminates near the root of the wing and landing gear components.

National Aerospace Laboratory NLR
Anthony Fokkerweg 2, 1059 CM Amsterdam,
P.O. Box 90502, 1006 BM Amsterdam, The Netherlands
Telephone +31 (0)88 511 31 13, Fax +31 (0)88 511 32 10, www.nlr.nl

Static and Fatigue Behaviour of Impact Damaged Thick-Walled Composites

R.J.C. Creemers and M.J. Smeets[1]

[1] Fokker Landing Gear B.V.

Customer

NL Agency

April 2014

This report is based on a presentation held at the RTO Workshop, Riga, Latvia, October 2013

The contents of this report may be cited on condition that full credit is given to NLR and the authors.

This publication has been refereed by the Advisory Committee AEROSPACE VEHICLES.

Customer	NL Agency
Contract number	59902N
Owner	NLR + partner(s)
Division NLR	Aerospace Vehicles
Distribution	Unlimited
Classification of title	Unclassified
Date	April 2014

Approved by:

Author	Reviewer	Managing department
R.J.C. Creemers	P. Nijhuis	H.G.S. J. Thuis
Date 22-04-2014	Date 22/4/2014	Date 22-5-2014

Content

Abstract 5

1 Introduction 5

2 Impact Testing 6

2.1 Test Specimens 6

2.2 Inspection Techniques 6

2.3 Typical Impact Damage 7

2.4 Impact Application 8

3 Static Test Results 12

4 Fatigue Test Results 14

5 Conclusions 17

6 References 17

This page is intentionally left blank.

Static and Fatigue Behaviour of Impact Damaged Thick-Walled Composites

R.J.C. Creemers
NLR
Voorsterweg 31, 8316 PR Marknesse
THE NETHERLANDS
ralf.creemers@nlr.nl

M.J. Smeets
Fokker Landing Gear
Grasbeemd 28, 5705 DG Helmond
THE NETHERLANDS
mike.smeets@fokker.com

ABSTRACT

Thick composites, such as applied in highly loaded landing gear components, respond differently to an impact event than thin composites. In this study the damage formation due to impacts on thick composites is determined together with the consequences of this damage for the compression after impact strength under static and fatigue loading. In both loading cases failure is governed by fibre kinking/crippling of the 0° plies within a post-buckled sub-laminate. Under static loading this results in collapse of the entire specimen. Under fatigue loading a crack starts to develop in these plies, which grows across the width of the specimen until it reaches the edge of the delaminated area. Next, the crack and delamination grow together towards the free edge of the specimen until final failure occurs.

1.0 INTRODUCTION

Using the Resin Transfer Moulding (RTM) manufacturing technique, it has become possible to produce thick composite components in a cost-effective way. This enables the replacement of complex metal forgings, such as landing gear components, by composite components. For more than 10 years the National Aerospace Laboratory (NLR) and Fokker Landing Gear (FLG) are cooperating in technology development for application of thick-walled composites in landing gear components. These landing gear components are typically in a laminate thickness range of 20 to 50 mm (Figure 1). They are subject to damage tolerance criteria, and a large variety of impact threats can be distinguished, both with low and high velocity, e.g. tool drop, collision with ground vehicles, hail, runways debris or tyre debris.

Figure 1: Examples of composite landing gear components.
Left: F-16 drag brace. Right: NH90 trailing arm.

Test data from literature and past test results seemed to indicate that aircraft structures made of thick composites material are less vulnerable to impact damage than thin composites (Ref. 1, 2 and 3). This would allow for the application of higher design strains in thick composite structures such as landing gear components, which would directly result in cost and weight savings. Therefore, a joint research programme was started by the NLR and FLG. The programme was partially funded by Agenschap NL and was performed in the framework of the Strategic Research Programmes.

In order to meet the objective of increased design strains for thick composites, it must be shown that the Compression Strength After Impact (CSAI) is higher than for thin composites. The static design strain for thin composites is so low (typically ~3000 με), that fatigue is usually not an issue in the design. However, when thick structures are allowed to operate at higher static strain levels, damage growth under fatigue loading might become critical. Therefore, both the static failure behaviour and the damage growth behaviour under fatigue were investigated.

2.0 IMPACT TESTING

2.1 Test Specimens

The test specimens used in the impact study were rectangular specimens with dimensions 190 mm x 100 mm x 20 mm and were cut from flat plates (Figure 2). The flat plates were manufactured by RTM using a uni-directional (UD) fabric with intermediate modulus fibres and a thermoset epoxy resin system. In a UD fabric the majority of fibres run in warp direction and only a small amount in weft direction. The plates are built up from 76 plies in total, and the majority of the plies is oriented in 0° direction resulting in a lay-up very close to a [60/30/10] ratio for the different fibre angles [0/±45/90]. The 0° direction is in length direction of the specimen, which is also the direction of the compressive loading during the static and fatigue tests. Because the specimens were also used to investigate the damage visibility of different impact events (Ref. 4), the specimens were painted white using the same coating as for current metal landing gear components.

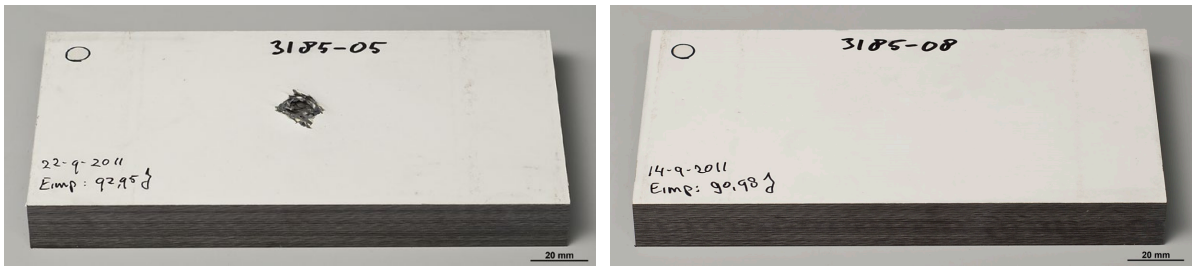

Figure 2: Rectangular specimens used for impact tests (90 J) with different speeds and impactors.

2.2 Inspection Techniques

Ultrasonic C-scanning was used to determine the amount of internal damage in the impacted specimens. Delamination damage is usually well detected by C-scan. However, a larger delamination may cover underlying smaller delaminations, which can no longer be found. Therefore, Time-Of-Flight (TOF) C-scan pictures were taken from both front and back side giving more information than the usual (one-sided) attenuation and reflection scan. Nevertheless, this still does not give a complete image of the internal delaminations. Also, using C-scan, voids can be found only to a certain extent, and transverse cracks and broken fibres generally go undetected. Therefore, to get a complete picture of the real internal damage, slices have been cut from some of the impact damaged specimens in order to inspect these under a microscope. To get a complete picture of the real internal damage some of these slices were cut from specimens directly after the impact event, others from specimens after being fatigue tested.

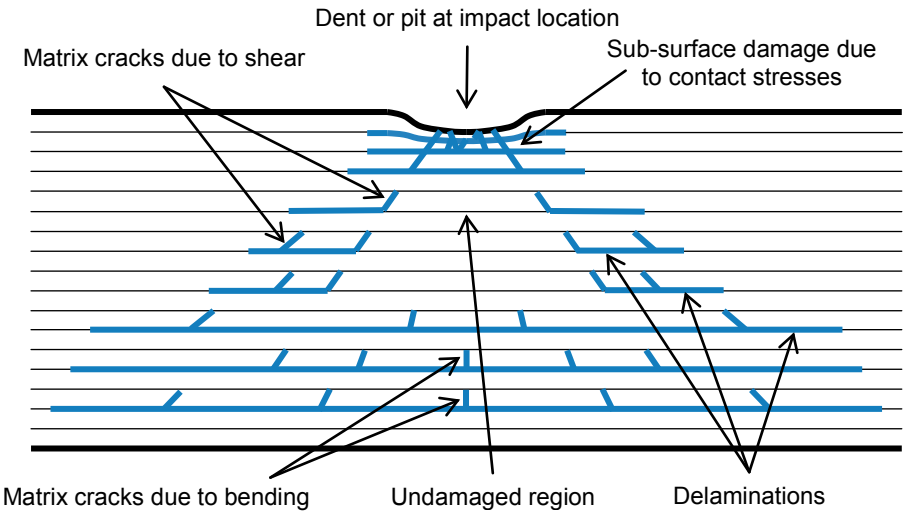

Figure 4: Internal damage found in the thick composite specimens (schematically).

2.3 Typical Impact Damage

Figure 4 gives a schematic view of the different types of damage that have been found in the thick composite specimens after being impacted. It is noted that in thin composites after impact it is common to find fibre breakage at the bottom side of the laminate due to a large amount of bending during impact. This fibre outbreak at the back of the laminate enables the development of a significant dent at the front side (Figure 5). In thick composites, however, fibre outbreak at the backside is generally not found after impact due to the high bending stiffness of the laminate, not even for impact energy levels exceeding 140 J. As a consequence, only a very shallow dent or, alternatively, a fairly deep pit is created (Figure 2). A pit is more likely to occur for a small hemispherical or sharp impactor (higher contact stresses) and for the high velocity impacts, because the maximum force for these impact events is larger. However, even with just an almost non-visible shallow dent in the top surface there is usually a lot of internal damage directly underneath the impact location in the form of matrix cracks and delaminations, sometimes accompanied by broken fibres. This sub-surface damage is caused by the (Hertzian) contact stresses that can become very high in an impact.

Below the region with sub-surface damage in the upper part of the specimen, there is a region where high shear stresses cause through thickness matrix cracks in the laminate. These cracks are formed under an angle, leaving a conically shaped region without damage directly under the impact location. Using the angles of the individual matrix cracks, it seems that they can be traced back to a single point just above the impact

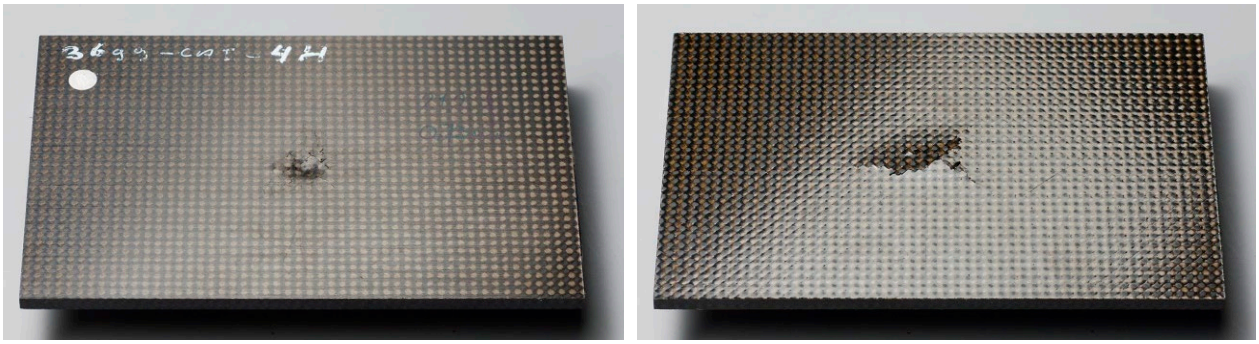

Figure 5: Impact on a thin 4 mm laminate. Left: dent at the front side caused by a 16 mm hemispherical impactor at 21 J. Right: outbreak at the back of the same sample.

location. The matrix cracks extend into delaminations that run outward, away from the impact location. In general, the delaminations run along the 0° fabric plies, either on top or below a cluster of 0° plies.

Below the central undamaged region large delaminations and matrix cracks are found. Away from the centreline, shear cracks occur in the matrix, similar to the matrix cracks in the central region. But near the centreline (directly underneath the impact location) transverse tensile cracks appear, which can be attributed to bending. Bending also causes the large delaminations in the bottom half of the specimen. Again, the delaminations primarily run along the 0° plies.

2.4 Impact Application

Many different impact tests have been performed by FLG. During the impact tests the specimens were clamped along their short sides, leaving a free span length of 110 mm. Four different types of impactors were used, hemispherical impactors with ½ inch and 1 inch diameter, and conical impactors with a nose angle of 60° and 120° (Figure 3). The impactor heads were made of aluminium. Both high velocity impacts using a gas cannon and low velocity impacts using a guided drop weight tower were performed with impact energy levels ranging from 12 J to 148 J. For the high velocity impacts the impactor head is slid into a plastic tubular housing (Figure 3), giving a total mass of 27.5 grams. For the low velocity impacts identical impactor heads were used but attached to a high mass of almost 3 kg.

In this paper only the static failure behaviour and damage growth behaviour under fatigue will be investigated for the most critical impact configurations:

- Configuration 1 – high velocity 140 J impact with the 1 inch hemispherical impactor;
- Configuration 2 – high velocity 90 J impact with the 1 inch hemispherical impactor;
- Configuration 3 – low velocity 140 J impact with the ½ inch hemispherical impactor.

These configurations were selected, because they combine a low detectability/visibility with the most detrimental type of damage for compression loaded specimens. The internal damage for the second impact configuration (90 J, high velocity, 1 inch impactor) is more or less similar to the damage pattern for the third impact configuration (140 J, low velocity, ½ inch impactor) and is therefore used for comparison.

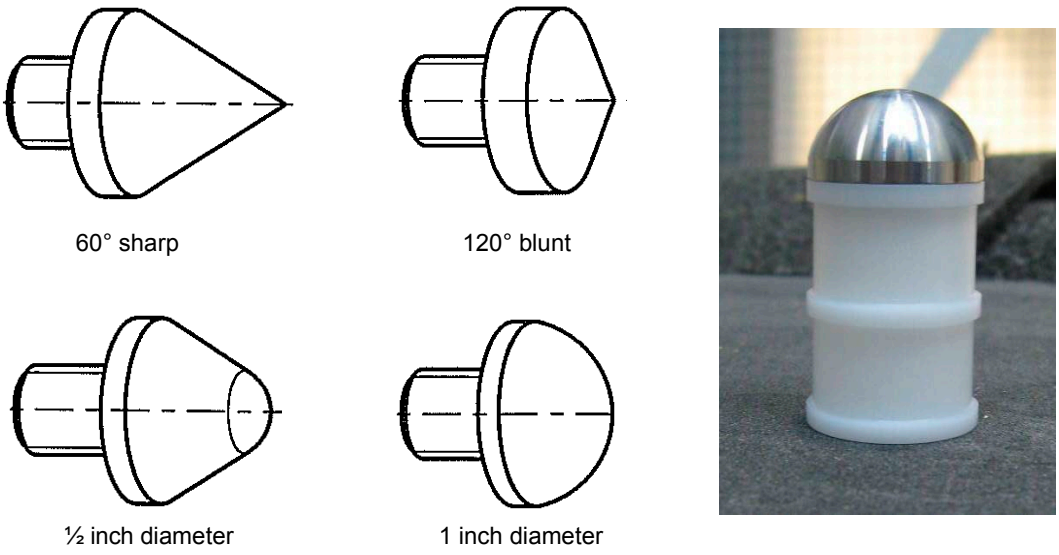

Figure 3: Different shapes used for the head of the impactor.

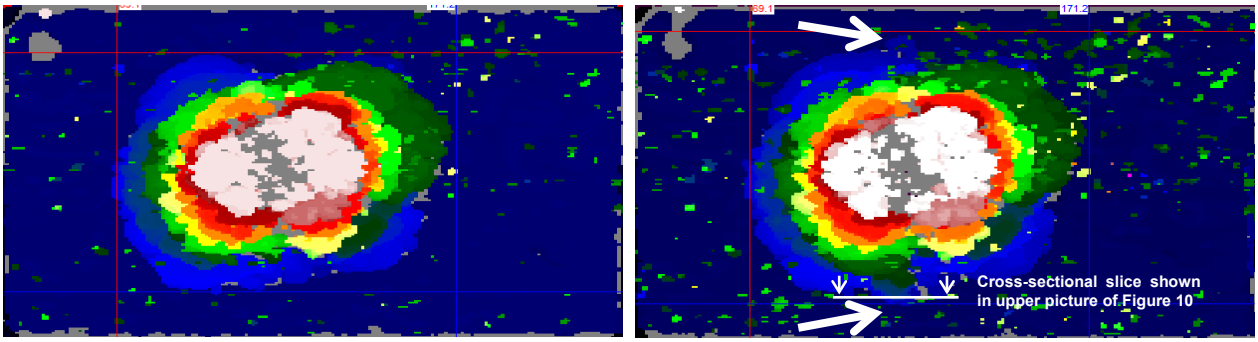

Figure 6: C-scans of impact damaged specimen (1 inch high speed 140 J). Left: before fatigue. Right: after 2,000 cycles. Large white arrows indicate sites with damage growth. Cross-sectional slices of this specimen are given in Figure 10.

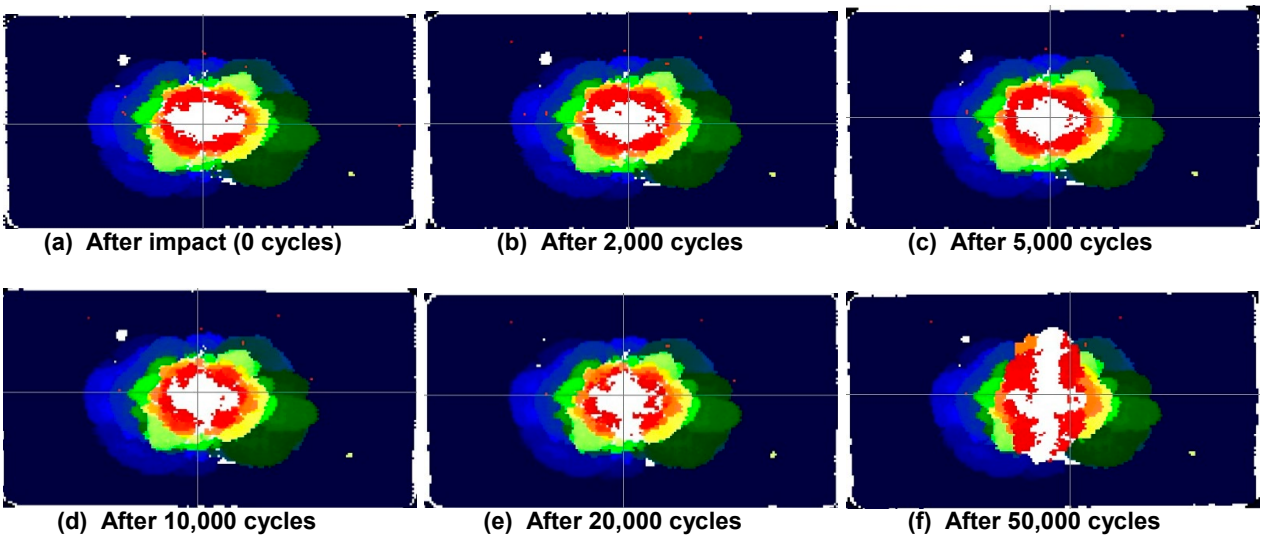

Figure 7: C-scans of impact damaged specimen (1 inch high speed 90 J) loaded in fatigue.

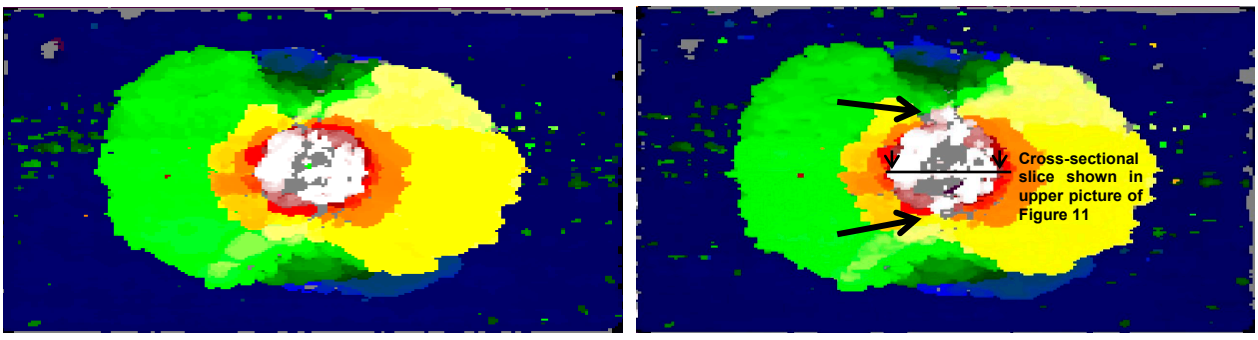

Figure 8: C-scans of impact damaged specimen (½ inch low speed 140 J). Left: before fatigue. Right: after 1,500 cycles. Black arrows indicate sites with damage growth. Cross-sectional slices of this specimen are given in Figure 11.

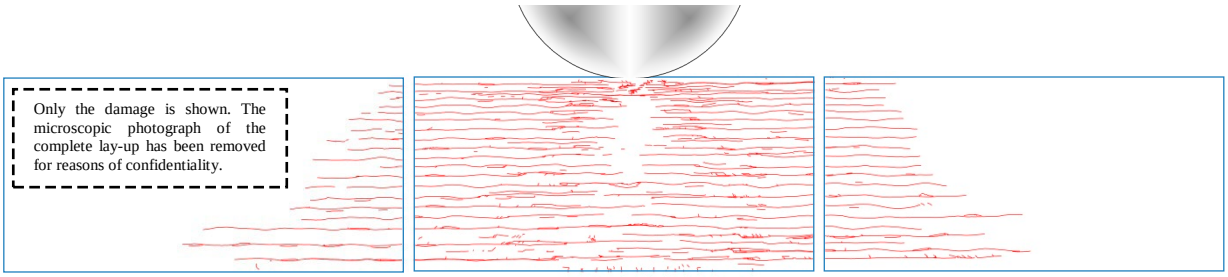

Figure 9: Slice through the centre of a specimen containing 1 inch high speed 140 J impact damage. No fatigue loading was applied to this specimen.

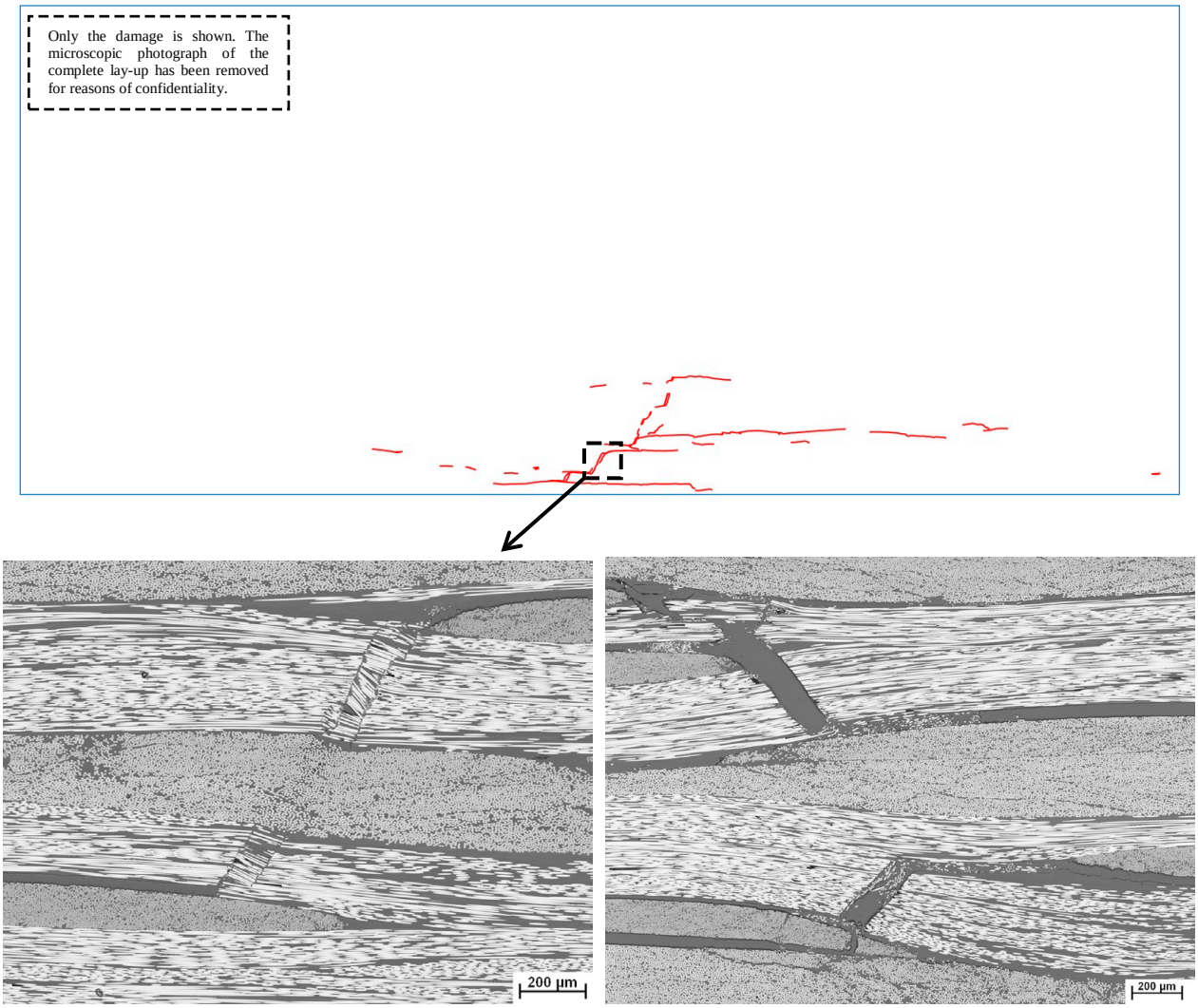

Figure 10: Microscopic photographs of a specimen containing a 1 inch high speed 140 J impact after fatigue loading. Upper: slice through the delamination boundary after growth as indicated in Figure 6. Lower left: detailed image showing kink bands in the 0° fibres. Lower right: detailed image (deeper inside the laminate) showing kink bands being pulverised and migrating into the open delamination.

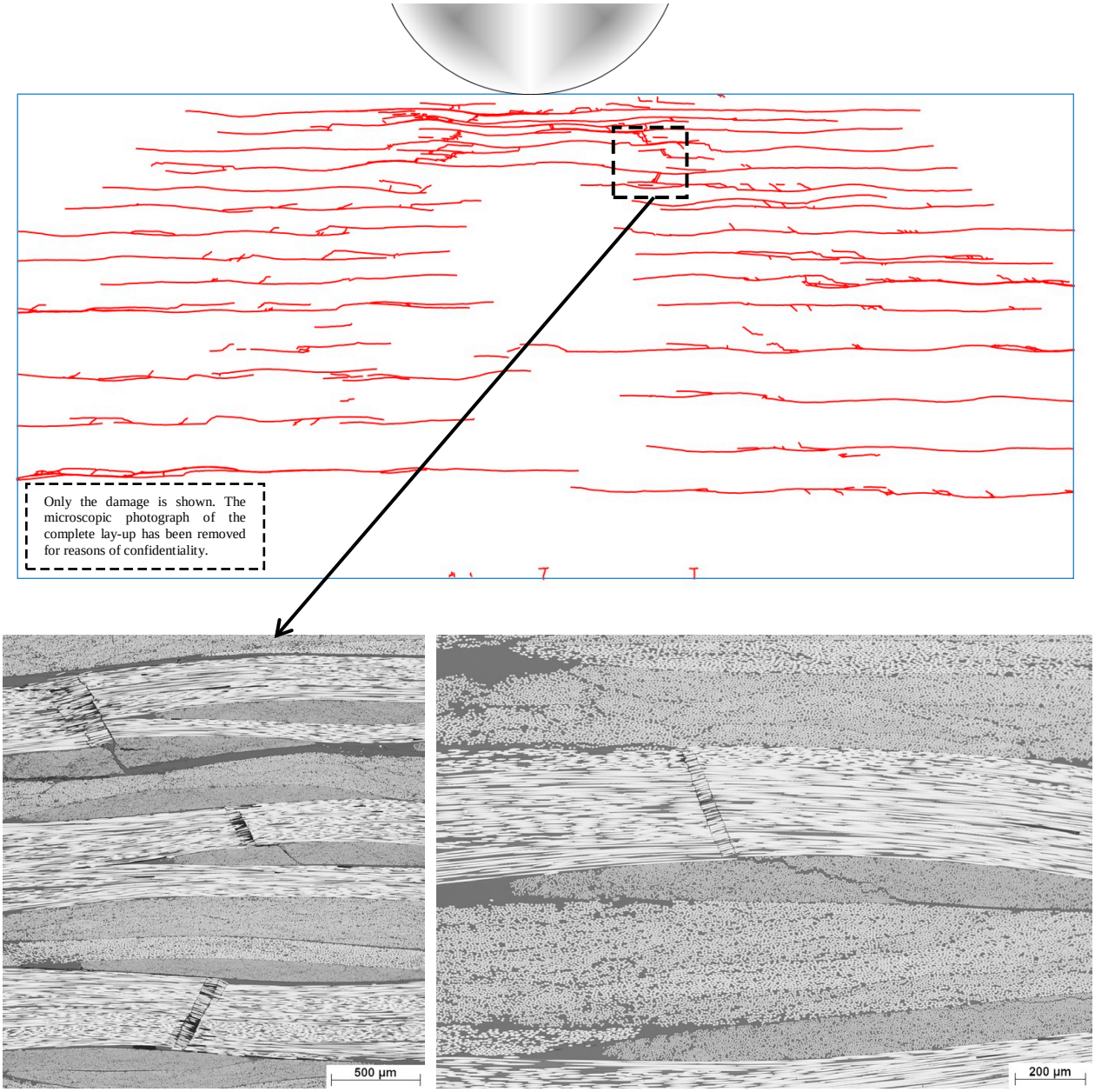

Figure 11: Microscopic photographs of a specimen containing a ½ inch low speed 140 J impact after fatigue loading. Upper: slice through the centre of the specimen as indicated in Figure 8. Lower left: detailed image showing kink bands in the 0° fibres. Lower right: detailed image of a very fine kink band near the top surface at the location of the upper black arrow in Figure 8.

For none of the critical impact configurations the specimens contain a pit at the front side. Besides some damage to the paint, which is chipped off for the ½ inch impactor (configuration 3) and cracked or blistered for the 1 inch impactor (configuration 1 and 2), there is hardly any damage visible from the outside. However, all specimen configurations contain a lot of internal damage. The C-scans reveal large delaminations in all specimen configurations (Figure 6-8). The C-scans also show that the damage pattern is somewhat different for the 140 J high speed impact with 1 inch impactor (configuration 1), where the delaminations at the front side are significantly larger and the delaminations are more closely stacked through the entire laminate, than for the other two configurations. This is confirmed by cross-sections that were made through these specimens (Figure 9-11). When compared to the 140 J impact with 1 inch impactor (configuration 1), the specimens impacted with the ½ inch impactor (configuration 3) contain relatively small delaminations just below the front surface, and towards the back the delaminations are not as closely

stacked as for configuration 1, leaving somewhat thicker sub-laminates in the lower half of the specimen. In chapter 3.0 it will be shown that this has a profound effect on the static test results.

3.0 STATIC TEST RESULTS

The impact damaged specimens are loaded statically to failure in compression. Figure 12 shows such a specimen after failure. The test is displacement-controlled with a loading rate of 0.2 mm/min. The following quantities have been measured during the static tests:

- Cross-head displacement and load by the test bench;
- Displacement between the two loading platens using an LVDT;
- The out-of-plane deflections using two laser displacement sensors, one at the front and one at the back.

The two lasers are used to capture any sub-laminate buckling prior to final failure. For a limited number of specimens the lasers were replaced by a 3D Digital Image Correlation (DIC) system to monitor the out-of-plane deflections and to obtain the entire strain field in the specimen, simultaneously at front and back.

Figure 13 shows the DIC measurements on a specimen containing damage due to a 140 J high speed impact with the 1 inch impactor (configuration 1). It can be seen that the out-of-plane deflections and the strains in the middle of the specimen show a strong increase beyond a certain point. Prior to failure the large sub-laminate at the back bends outward while the smaller sub-laminate at the front bends inwards, so in the same direction as the sub-laminate at the back. Thus, the entire stack of thin sub-laminates must be bending/buckling towards the back of the specimen. This behaviour is confirmed by the strain data. At both the front and back side strain concentrations are found but with an opposite pattern, indicating that (indeed) the front delamination is bending inward and the back delamination outward. Failure itself is a very sudden event without any cracking sounds or sudden changes in the strain measurements, which indicates that no delamination growth occurs before final failure. In total four specimens of this configuration have been tested statically, with the lowest failure load at 99% and the highest at 102% of the average failure load, so the amount of scatter is very limited.

The measurements on the configurations 2 and 3, i.e. the 1 inch high speed 90 J impact and the ½ inch low speed 140 J impact, reveal that the buckling behaviour of these two configurations is entirely different compared to the 1 inch high speed 140 J impact. The static measurements reveal that for configurations 2 and 3 the large but thick sub-laminates near the back do not bend away prior to failure, while the small but thin sub-laminates near the front buckle outward. This different behaviour can be traced back to the damage

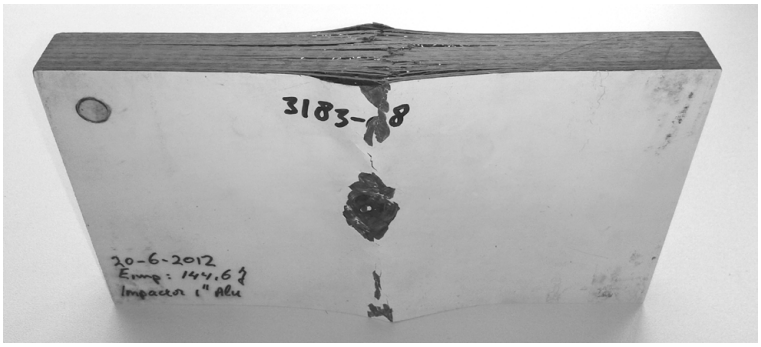

Figure 12: Specimen with a 1 inch high speed 140 J impact after static failure.

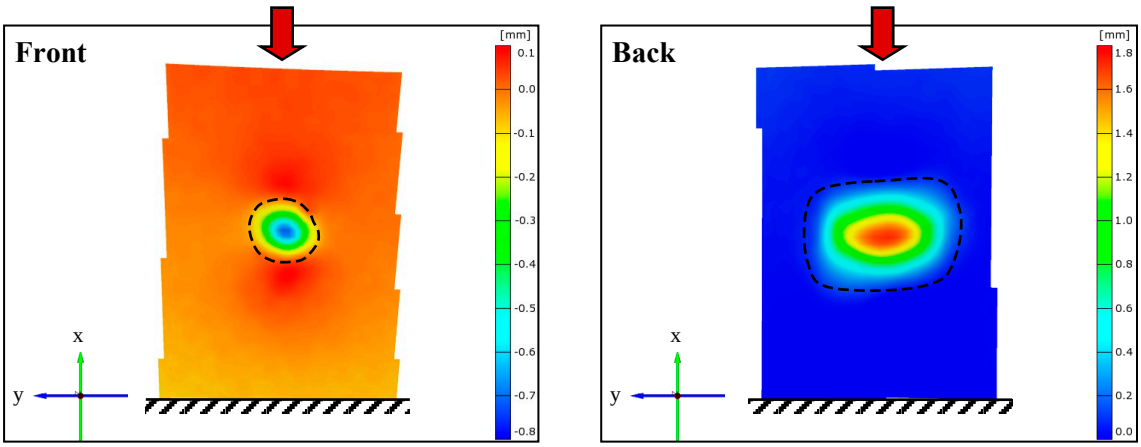

(a) Out-of-plane displacements (δ_z).

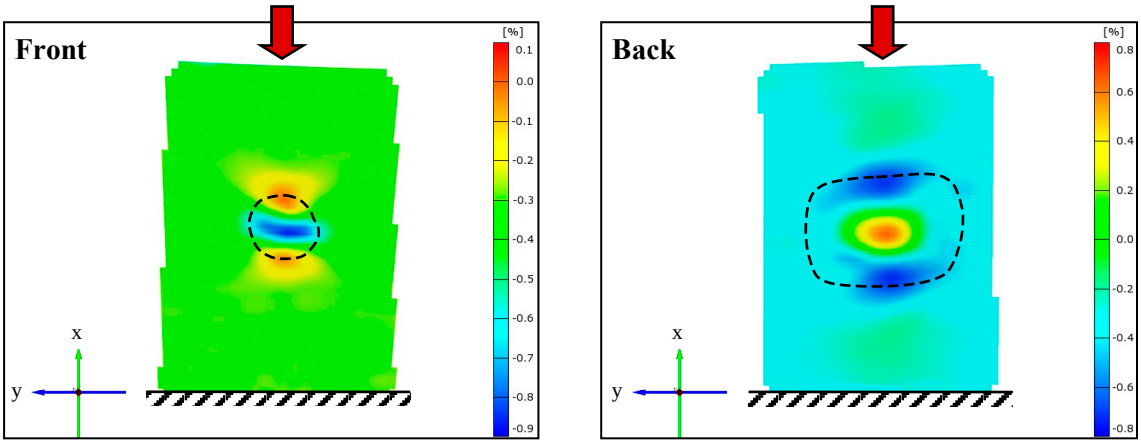

(b) Strains in loading direction (ε_x).

(c) Strains in loading direction (ε_x) vs. applied load.

Figure 13: DIC measurements for a specimen containing a 1 inch high speed 140 J impact.

pattern. For all configurations the impact created large delamination damage near the back and smaller delaminations near the top surface, but cross-sections through the specimens (Figure 11) show that the separate sub-laminates in configurations 2 and 3 are fairly thick compared to configuration 1; only the sub-laminates directly underneath the front surface are quite thin, allowing only buckling of the front delaminations in outward direction. For the specimens with the ½ inch low speed 140 J impact (configuration 3) DIC measurements confirm this outward buckling of a small sub-laminate at the front. The DIC results are not presented here, but they show that strong strain concentrations exist at the front, both in the loading direction and perpendicular to the loading direction, which corresponds to the deformation of a small sub-laminate buckling outward. At the back of the specimen the strains remain uniform in the entire

specimen. Only two specimens of this configuration 3 were tested statically. For configuration 2 the behaviour is similar to configuration 3, with a 10% less average failure load.

The DIC strain measurements of Figure 13 show that there is hardly a “soft inclusion” or “open hole” effect with evident stress/strain concentrations next to the damaged area. However, within the damaged area very high local strains occur due to buckling of sub-laminate(s). In fact, the amount of bending and curvature of these buckled sub-laminates is so high that despite the specimen being loaded in compression the strains in loading direction even become tensile (and high!) at the outer surface. This can only mean that, internally, even higher compressive strains occur than the tensile values observed at the outside. With compressive strain levels well beyond 7000 με, it is very likely that in a static strength test final collapse of the specimen is initiated by compression failure of the load-carrying 0° fibres in such a post-buckled sub-laminate; the “far field” strains may be low, but locally very high strain levels occur.

4.0 FATIGUE TEST RESULTS

Fatigue tests have been performed on the three specimen configurations of paragraph 2.4, the 1 inch high speed 140 J impacts, the 1 inch high speed 90 J impacts, and the ½ inch low speed 140 J impacts. The specimens are loaded in fatigue at different stress/strain levels in order to create an S-N curve. All fatigue tests have been performed in compression-compression with R=10 at 3 Hz. Before the fatigue test was started, the specimens were C-scanned to obtain a baseline scan. During fatigue the test was stopped at specific intervals and the specimens were C-scanned again to detect any growth of damage before the final failure of the specimens. In general, the following inspection scheme has been followed:

$$0,\ 100,\ 200,\ 500,\ 10^3,\ 2\cdot10^3,\ 5\cdot10^3,\ 10^4,\ 2\cdot10^4,\ 5\cdot10^4,\ 10^5,\ 2\cdot10^5,\ 5\cdot10^5,\ 10^6,\ 2\cdot10^6,\ 3\cdot10^6 \text{ cycles}$$

The fatigue test was finished when the specimen failed or after 3 million cycles. Sometimes it was decided to stop the test prior to final failure when damage growth was detected by the C-scan. However, during the fatigue test programme it became clear that by the time the delaminations started to grow, the impact damage had already grown in another mode which went undetected by the C-scans. This is shown below.

Figure 6 to 8 show C-scans of the three specimen configurations during the fatigue tests. For configuration 1, i.e. 1 inch high speed 140 J impact, and configuration 3, i.e. ½ inch low speed 140 J impact, the fatigue test was stopped immediately after the first detection of growth, so the amount of damage growth visible on the C-scans is very limited (Figure 6 and 8). For configuration 2, i.e. 1 inch high speed 90 J impact, the damage was allowed to grow until it resulted in final failure, so much more extensive growth is visible on the C-scans of Figure 7. The damage grows across the width of the specimen perpendicular to the loading direction. The C-scans show that it is essential to make TOF pictures, because it is possible that growth of the small delaminations at the front side occurs first, before growth of the large delaminations at the back, see Figure 7 and 8. This would have gone undetected when only the total enclosed delamination area in an attenuation or reflection scan would have been examined, because the large delaminations at the back cover the smaller delaminations at the front until the damage grows beyond the largest delamination, which happens only just before final failure. The C-scans show that the same subdivision for the damage growth behaviour can be made as for the failure behaviour in the static tests. The specimens with the 1 inch high speed 90 J impact (configuration 2) and the ½ inch low speed 140 J impact (configuration 3) behave similarly with damage growth initiating at the smaller delaminations at the front. The behaviour of configuration 1, i.e. the specimen with the 1 inch high speed 140 J impact, is entirely different with damage growth initiating at the larger delaminations at the back. So, damage growth occurs at the same location as where buckling initiated in the static tests. Furthermore, buckling of such a sub-laminate (either at the front or at the back) is clearly visible in the fatigue tests Therefore it is suspected that, despite the seemingly different behaviour of the different specimen configurations, the underlying damage growth mechanism is actually the same. This suspicion is confirmed by a more detailed investigation of the damage growth behaviour.

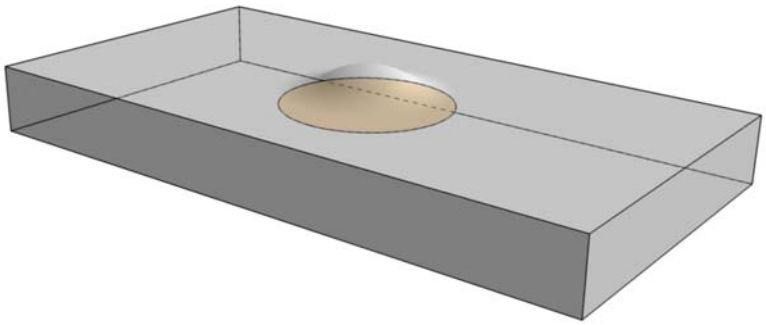

(a) Buckling/bending of a sub-laminate.

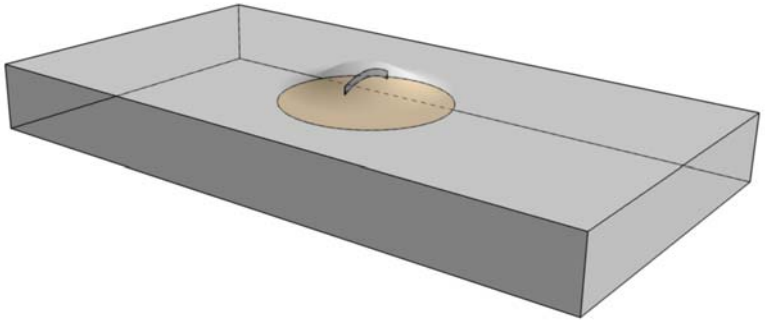

(b) Initiation of a crack in the 0° plies (due to fibre kinking).

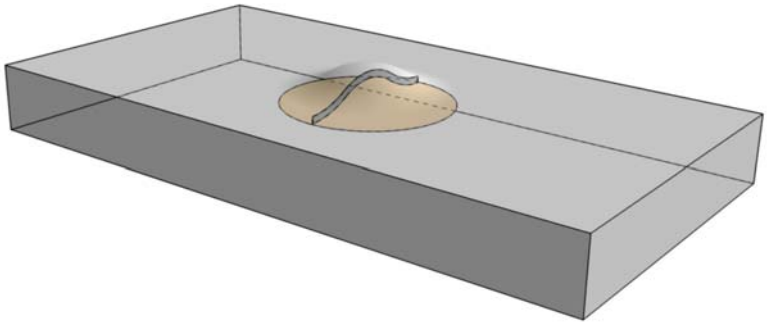

(c) Growth of the crack until it reaches the edge of the delamination.

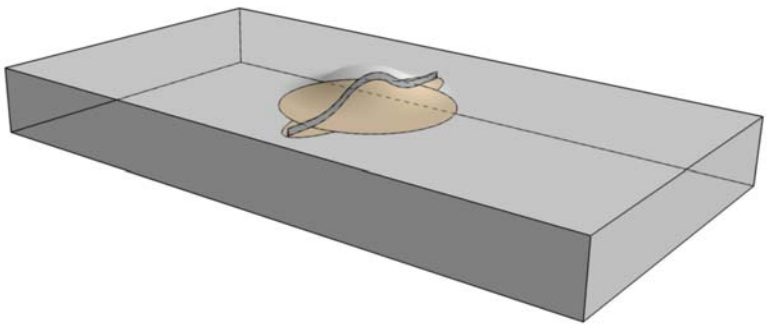

(d) Combined/simultaneous growth of the crack and delamination.

Figure 14: Schematic representation of the different stages of damage growth due to fatigue.

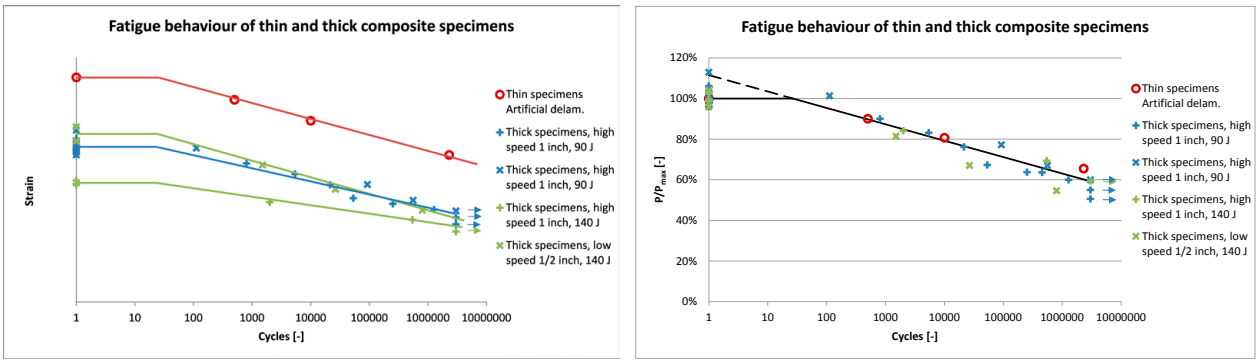

Figure 15: S-N curves for impact damaged thick composite specimens and for thin composite specimens with artificial delaminations. Left: compressive strains. Right: normalised strength.

The first detection of damage growth is established by ultrasonic C-scan and growth may occur at the large delaminations near the back or at the small delaminations near the front. However, the cross-sections of Figure 10 and 11 through the fatigue tested specimens show that in the meantime an internal fibre crack has already developed in the load-carrying 0° plies of one or more sub-laminates. Figure 10 (configuration 1) shows a slice that was made right at the lower boundary of the large dark blue delamination in Figure 6, more to the side of the specimen, through the small lobe with delamination growth. Several 0° plies towards the back side are cracked and a detailed picture of such a crack shows distinct kink bands in the 0° fibre bundles indicating a compressive failure mode. Slices more to the centre of the delaminated area reveal that the fibre crack is present across the entire width of the delaminated area, and that the delaminations are very opened up while the cracks in the 0° plies are characterised by large gaps. The fine kink bands that can be found at the ends of the crack (near the delamination boundary) have been pulverised in the centre of the delaminated area by the constant fatigue loading, and these kink bands migrate into the open delamination (bottom right picture of Figure 10) until they have completely disappeared leaving a gap behind. Figure 11 (configuration 3) shows identical failures, i.e. distinct kink bands (and/or gaps) in the 0° plies in the centre line of the specimen that become finer and finer towards the edge of the crack. However, the crack is now located towards the front (impact) side of the specimen and the tip of the crack stops at the boundary of the small delamination. With a crack present across the entire width of the delaminated area (either at the front or at the back) and only the slightest amount of delamination growth, it must be concluded that damage growth actually starts with a crack progressing across the width of the delaminated area perpendicular to the loading direction. This crack, however, is not visible from the outside nor is it detected by C-scan. To find those cracks it is necessary to end the fatigue test and to cut slices in length direction through the specimen (micro-CT-scan would also be capable to detect such a crack during the test, but the very fine kink bands would probably still go undetected). So, with conventional non-destructive inspection techniques such a crack remains undetected until it reaches the edge of the delaminated area. Next, both crack and delamination grow outwards together and the advancing delamination front is eventually detected by C-scan. This damage growth mechanism is shown schematically in Figure 14.

The current fatigue test results and additional fatigue tests on thin 4 mm specimens with artificial delaminations show that a crack is actually required first, before delamination growth occurs. Without the crack in the load-carrying 0° plies the delaminations would not have grown (as in the classical mode I/II delamination growth). The location where such a crack develops is directly related to the (local) bucking behaviour of the specimen. If a small but thin sub-laminate at the front buckles first, the increased bending strains will cause crack growth near the front. If a larger but possibly thicker sub-laminate at the back buckles first, crack growth will also initiate near the back. So, this shows that both static failure and fatigue failure are most likely governed by the same failure mechanism, i.e. compressive failure of the load-carrying 0° plies of a sub-laminate that is bending or buckling outward. The buckling load and mode (and therefore also the static failure load and fatigue strength) depend entirely on the damage pattern in the impact damaged specimens which explains why sometimes damage growth occurs at the front and sometimes at the back. When the damage mechanisms are coupled the fatigue strength might also be related to the static strength.

This is examined in Figure 15. The left picture shows that there is quite some difference in the absolute static and fatigue strength of the different specimen configurations. However, when the fatigue strength is normalised for the static strength the test points converges to one single curve for all the different configurations, even for the specimens with artificial delaminations. This is another indication that only one single damage mechanism (fibre kinking/crippling) is the cause for both static failure and fatigue damage growth and that it is not initiated by the classical delamination growth in mode I or II.

5.0 CONCLUSIONS

The creation of damage due to an impact event is different for thick composites compared to thin composites. The large bending stiffness prevents fibre break-out at the back surface and therefore also the creation of a significant dent at the front surface. Instead, a pit/hole is created right at the impact location where the impactor penetrates the top surface, or alternatively only a very shallow dent occurs in combination with a large amount of internal damage consisting of sub-surface contact damage, shear cracks in the upper half of the specimen extending into delaminations, and very large delaminations due to bending in the lower half of the specimen. In this paper the static failure behaviour and damage growth behaviour under fatigue was investigated for the three most critical impact configurations only, because they combine a very low detectability/visibility (shallow dent) with the most detrimental type of damage for compression loaded specimens (large delaminations).

Depending on the type of impact, the static strength can be quite low and the objective of increased design strains for thick composites cannot be met when using dent depth as damage visibility criterion. The large amount of internal delamination damage leads to local sub-laminate buckling prior to failure, either at the front or at the back depending on the damage pattern in the specimen. This results in locally very high (bending) strains in the post-buckled sub-laminates. The high compressive strains in the load-carrying 0° plies are the most likely cause for final failure through fibre kinking/crippling. Failure itself is a very sudden event without any stiffness decrease or cracking sounds that might indicate damage growth prior to static failure.

Under fatigue loading, damage growth initiates in the same mode as final failure in the static test specimens. Again, damage growth starts by fibre kinking of the load-carrying 0° plies within a (post-buckled) sub-laminate at the front or back. Buckling/bending increases the strains in such a sub-laminate and promotes the initiation of a crack under fatigue loading. Next, this crack grows across the width of the sub-laminate until it reaches the edge of the delaminated area. And finally, the crack and delamination grow together towards the free edge of the specimen.

So, for the current specimens the failure behaviour is not at all governed by the classical mode I/II delamination growth. Instead, both static and fatigue failure are governed by a fibre-dominated failure mode, and the fatigue strength can be directly related to the static strength with the fatigue limit (or 3 million cycles) at a fixed ratio of approximately 60% of the static strength. Consequently, when a probability analysis is able to show that a lower impact energy cut-off level can be applied than the current 140 J, the fatigue limit will increase together with the static design strain.

6.0 REFERENCES

[1] J. Bauer, G. Günther, R. Neumeier, Allowable Compression Strength for CFRP-Components of Fighter Aircraft Determined by CAI-Test, AGARD Conference Proceedings, AGARD-CP-530, May 1992.

[2] A.P. Marshall, H. Bouadi, Low-Velocity Impact Damage on Thick-Section Graphite/Epoxy Laminated Plates, Journal of Reinforced Plastics and Composites, Vol. 12, Number 12, pp. 1281-1294, 1993.

[3] C.E.P. Breen, F.J. Guild, M.J. Pavier, Impact damage to thick carbon fibre reinforced plastic composite laminates, Journal of Materials Science, Vol. 41, Number 20, pp. 6718-6724, 2006.
[4] J.H. Heida and J.M. Müller, In-service Inspection and Monitoring of Composite Aerospace Structures, STO-MP-AVT-224, PAPER NBR 4.

WHAT IS NLR?

The NLR is a Dutch organisation that identifies, develops and applies high-tech knowledge in the aerospace sector. The NLR's activities are socially relevant, market-orientated, and conducted not-for-profit. In this, the NLR serves to bolster the government's innovative capabilities, while also promoting the innovative and competitive capacities of its partner companies.

The NLR, renowned for its leading expertise, professional approach and independent consultancy, is staffed by client-orientated personnel who are not only highly skilled and educated, but also continuously strive to develop and improve their competencies. The NLR moreover possesses an impressive array of high quality research facilities.

***NLR** – Dedicated to innovation in aerospace*

www.nlr.nl